Synthesis and QSAR of Herbicidal 3-Pyrazolyl α,α,α-Trifluorotolyl Ethers

Robert D. Clark*

Monsanto Company, 800 North Lindbergh Boulevard, St. Louis, Missouri 63167, and Tripos, Inc., 1699 South Hanley Road, St. Louis, Missouri 63144

Pyrazole nitrophenyl ethers (PPEs) were recently identified as a novel class of chemistry exerting herbicidal effects by inhibition of protoporphyrinogen IX oxidase. This area of chemistry has been extended to include herbicidal pyrazolyl fluorotolyl ethers. In these compounds, a trifluoromethyl group substitutes for the 4′-nitro group found in the original herbicides and in "classical" nitrodiphenyl ether hebicides. Fluoroanisole pyrazole ethers, in which a trifluoromethoxy group replaces the nitro group of diphenyl ether herbicides, are also described. The shift from 4′-nitro to 4′-trifluoromethyl substitution, which is conservative in terms of electrostatics, produced a novel class of herbicide with substantial pre-emergent activity on narrowleaf weed species. Quantitative structure/activity relationships obtained with respect to substitution on the pyrazole ring and at the 3′-position of the fluorotolyl moiety can be summarized effectively by comparative molecular field analysis. In general, 5-methanesulfonyl fluorotoluidide ethers were found to be most active.

Keywords: *Herbicide; protoporphyrinogen oxidase; structure/activity; QSAR; pyrazole phenyl ether; comparative molecular field analysis; CoMFA*

INTRODUCTION

A new class of herbicides generically designated pyrazole phenyl ethers (PPEs) were recently discovered by Monsanto Co. (Rogers and Moedritzer, 1990; Moedritzer *et al.*, 1992). These compounds act by inhibiting protoporphyrinogen oxidase (Sherman *et al.*, 1991; Nandihalli *et al.*, 1994), as do structurally related nitrodiphenyl ethers (nitroDPEs). Analog synthesis in this area dealing with pyrazolyl *p*-nitrophenyl ethers, which can be characterized by the generic structure **1** (Figure 1), has been described elsewhere (Rogers and Moedritzer, 1990; Moedritzer *et al.*, 1992). However, the extensive DPE patent literature is replete with claims of herbicidal activity for compounds in which the nitro group of "classical" DPEs such as acifluorfen and oxyfluorfen is replaced by a halogen or pseudohalogen. In several cases, trifluoromethyl has been included in the claims, but full exposition of synthetic details for such compounds [e.g., Barton *et al.* (1988)] is rare, particularly for nontrivial, substituted analogs. Trifluoromethoxy as a nitro replacement is better documented (Hiraga *et al.*, 1980) and was also of interest.

This scarcity of well-documented examples may reflect the difficulty of working with *p*-(trifluoromethyl)-phenol, which would be necessary if one were to follow synthetic routes analogous to those most commonly used to prepare most DPEs (Clark, 1994). The alternative of reduction, diazotization to the iodide, and reaction with trifluoromethylzinc (Barton *et al.*, 1988) is limited in scope and does not readily lend itself to extensive analog synthesis. The trifluoromethyl zinc procedure fails, in particular, for PPEs. The Monsanto herbicides, however, are prepared by coupling of *p*-nitrophenyl halides with 3-hydroxypyrazoles. This makes benzotrifluoride analogs more directly accessible for PPEs than for DPEs.

Generic structures for herbicidally active pyrazolyl fluorotolyl ethers described here (**2**−**16**) are given in Figure 1; several fluoroanisole ethers (**17**−**19**) are included as well. The corresponding physical data are presented in Table 1. Table 2 sets out the relative potencies found, with the compounds arranged in order of decreasing herbicidal activity.

* Address correspondence to the author at Tripos, Inc. [telephone (314) 647-1099; fax (314) 647-9241; e-mail bclark@tripos.com].

GENERAL SYNTHETIC METHODOLOGY

Physical properties of analogs covered in this paper are given in Table 1. Melting points cited are not corrected. ^{1}H NMR spectra were obtained at 300 (Varian XL-300 or IBM AF-300), 360 (Bruker AM-360), or 400 MHz (Varian XL-400), whereas ^{13}C spectra were obtained at 75, 90, or 100 MHz. ^{19}F spectra were collected at 282 or 339 MHz. The solvent used was deuteriochloroform unless otherwise noted, and multiplicities and integrals of unity have been omitted in the interests of brevity. ^{1}H chemical shifts are in parts per million (δ) with respect to tetramethylsilane, whereas ^{19}F chemical shifts are cited with respect to fluorotrichloromethane.

Ultraviolet spectra were obtained on a Beckman DU-7 spectrophotometer in methylene chloride. Coupled GC/MSD analyses were run on a Hewlett-Packard 58900 gas chromatograph equipped with a 12.5 m × 0.2 mm cross-linked dimethyl silicone capillary column and an HP 5970 mass-sensitive detector. Satisfactory elemental analyses (Atlantic Microlabs, Inc., Norcross, GA) were obtained for all compounds cited.

Most analogs were accessible from *o*- (Scheme 1) or *m*- (Scheme 2) nitrophenyl ethers (Scheme 2). Preparation of *N*″-substituted toluidine ethers (Scheme 3) presented special challenges, as did preparation of trifluoromethoxy analogs (Scheme 4). Unless otherwise noted, inorganic chemicals and reagent grade solvents were obtained from Fisher and organic reagents and anhydrous solvents from Aldrich. Yields cited have not been optimized unless noted to the contrary. HPLC was carried out on a Waters Prep 500, radial chromatography was run on a Model 7924 Chromatotron (Harrison Research), and Davisil 633/60A silica gel served as adsorbent for flash chromatography.

Via *o*-Nitrophenyl Ethers (Scheme 1). 5-(Methythio)- or 5-(trifluoromethyl)-3-hydroxypyrazole **21** or **20**, respectively (Moedritzer *et al.*, 1992), was coupled with a substituted fluorobenzene activated for aromatic nucleophilic substitution by an *o*-nitro group. This superfluous nitro group was subsequently reduced by catalytic hydrogenation or with iron in acetic acid, and the product was deaminated using *tert*-butyl nitrite in dimethylformamide (Doyle *et al.*, 1977). Aqueous

S0021-8561(96)00197-5 CCC: $12.00

Table 1. Physical Properties of Herbicidal 3-Pyrazolyl α,α,α-Trifluorotolyl Ethers

compd	Q [Z[a]]	mp (°C)	yield (%)	NMR	GC/MS
2a	H	46−48	73	^{1}H: δ 3.98 (3H), 6.35 (C^4H), 7.49 (dd), 7.69 (d, 2.4 Hz), 7.81 (d, 8.8 Hz)	
2b	Br	79−80	90	^{1}H: δ 3.99 (3H), 6.67 (d), 7.45 (dd), 7.81 (d)	
2c	Cl	82−83.5	63	^{1}H: δ 4.01 (3H), 7.50 (dd), 7.72 (d, 2.4 Hz), 7.85 (d, 8.8 Hz)	
3a	H	36−38	56	^{1}H: δ 3.83 (3H q, 1.1 Hz), 7.11 (2H ∼d, 9.0 Hz), 7.52 (2H ∼d, 9.1 Hz) ^{13}C: δ 39.2, 118.7 (q, 271 Hz), 117.0 ($C^{2'(6')}$H), 125.7 (q, 42 Hz), 126.7 (q, 3.7 Hz, $C^{3'(5')}$H), 153.8, 158.0, 175.4 ^{19}F: δ −62.0 (∼tr, 0.6 Hz, $C^{4'}CF3$), −59.4 (q, 0.9 Hz, C^5CF_3)	
3b	Br	oil	56	^{1}H: δ 3.88 (3H), 7.06 (dd, 8.6 & 1.8 Hz), 7.39 (d, 2.4 Hz), 7.58 (d, 9.0 Hz) ^{19}F: δ −63.7, −61.4	
3c	Cl	yellow oil n_D = 1.4855	47	^{1}H: δ 2.36 (3H), 3.82 (3H), 7.31 ($C^{6'}$H), 8.29 ($C^{3'}$H) ^{19}F: δ −64.1	
4a	NH_2	58−62	97	^{1}H: δ 3.97 (3H), 4.27 (2H), 6.48 (2H m), 7.42 (d, 8.8 Hz) ^{19}F: δ −63.9 (d, 25 Hz, $C^{4'}CF_3$), −61.3 (C^5CF_3)	
4b	NHAc	138−141	95	^{1}H: δ 2.21 (3H), 3.94 (3H), 6.93 (d), 7.45 (br), 7.56 (d), 8.15 (br s)	
5a	NMeAc	105−105.5	79	^{1}H: δ 1.71 (3H), 3.10 (3H), 3.86 (3H), 6.93 (d), 7.17 (dd), 7.65 (d) ^{19}F: δ −62.6, −61.4	
5b	NHMe	90−91	27	^{1}H: δ 2.77 (3H d, 5.1 Hz, $C^{3'}NHC\mathbf{H}_3$), 3.83 (3H, N1C$\mathbf{H}_3$), 4.34 (br, $C^{3'}N\mathbf{H}$Me), 6.24 (dd), 6.37 (d), 7.27 (d) ^{13}C: δ 30.3, 36, 39.5, 100.3, 101, 103.8, 109 (q, 37 Hz, $C^{3'}$NH), 119.1 (q, 271 Hz), 125.1 (q, 271 Hz), 128.2 (q, 5.6 Hz, $C^{5'}$H), 128.8 (q, 38 Hz), 148, 154.5, 160 ^{19}F: δ −63.9, −61.5	
6a	H	∼25 (160 °C at 1.5 Torr)	85	^{1}H: δ 2.41 (3H, SCH_3), 3.90 (3H, N^1CH_3), 7.17 (2H d), 7.58 (2H d, 8.6 Hz) ^{19}F: δ −63.6	
6b	CO_2Et	oil	68	^{1}H: δ 1.38 (3H tr), 2.41 (3H), 3.90 (3H), 4.38 (2H q), 7.26 (dd), 7.49 (d, 2.8 Hz), 7.69 (d, 8.8 Hz)	
6c	Cl	yellow oil n_D = 1.4120	61	^{1}H: δ 2.42 (3H), 3.91(3H), 7.05 (dd), 7.23 (dd), 7.63 (d) ^{19}F: δ −63.4	
6d	NO_2	76.5−78	65	^{1}H: δ 2.47 (3H), 3.96 (3H), 7.46 (dd), 7.66 (d, 2.0 Hz), 7.82 (d, 8.8 Hz) ^{13}C: δ 18.0 (SCH_3), 37.5 (N^1CH_3), 113.7, 120.4, 129.5 (q) ^{19}F: δ −60.8	
7	NHAc	155−156.5	79	^{1}H: δ 2.23 (3H), 2.45 (3H), 3.93 (3H), 6.93 (br d), 7.47 (br), 7.58 (d), 8.17 (br) ^{19}F: δ −61.2	
8	OMe	oil n_D = 1.5364	41	^{1}H: δ 2.39 (3H, SC$\mathbf{H}_3$), 3.86 (3H), 3.89 (3H), 6.60 (dd, 8.7 and 2.3 Hz), 6.76 (d, 2.3 Hz), 7.46 (d, 8.7 Hz) ^{13}C: δ 18.0 (SCH_3), 37.5 ($N^1\mathbf{C}H_3$) , 56.0 ($O\mathbf{C}H_3$), 101.8 ($C^{6'}$H), 104.2, 107.5, 114.0 (q, 3.4 Hz), 123.6 (q, 270 Hz), 128.2 (q, 5.3 Hz, $\mathbf{C}^{4'}CF_3$), 134.3, 153.8, 158.9 (q), 160.2 ^{13}C: δ 18.0 (SCH_3), 37.5 ($N^1\mathbf{C}H_3$) , 56.0 ($O\mathbf{C}H_3$), 101.8 ($C^{6'}$H), 104.2, 107.5, 114.0 (q, 3.4 Hz), 123.6 (q, 270 Hz), 128.2 (q, 5.3 Hz, $\mathbf{C}^{4'}CF_3$), 134.3, 153.8, 158.9 (q), 160.2 ^{19}F: δ −63.5 ^{19}F: δ −63.5	
9a	H	69−71	80	^{1}H: δ 3.15 (3H), 4.12 (3H), 7.24 (2H d), 7.65 (2H d) ^{19}F: δ −63.2	
9b	NO_2	127−128	76	^{1}H: δ 3.16 (3H), 4.14 (3H), 7.50 (dd), 7.72 (d), 7.85 (d) ^{13}C: δ 39.1, 40.1, 99.5 (C^4Cl), 114.1, 118.5 (q, 41 Hz, $\mathbf{C}^{4'}CF_3$), 120.7, 122 (q, 270 Hz, $C^{4'}CF_3$), 129.6 (q, 5.3 Hz), 138, 152.5, 158.5, 167, 188 ^{19}F: δ −61.0	
9c	NHAc	127−136	63	^{1}H: δ 2.30 (3H), 3.20 (3H), 4.17 (3H), 7.01 (d), 7.58 (br), 7.67 (d), 8.20 (br)	
10a	H	90−91.5	56	^{1}H: δ 3.32 (3H), 4.15 (3H), 7.25 (2H d), 7.66 (2H d)	
10b	CO_2Et	72−74	94	^{1}H: δ 1.39 (3H tr), 3.29 (3H), 4.12 (3H), 4.40 (2H q), 7.31 (ddq, 8.4, 2.4 and 0.8 Hz), 7.52 (d, 2.4 Hz), 7.73 (d, 8.4 Hz) ^{13}C: δ 13.9, 40.7, 44.5, 62.4, 102.7, 119.3, 119.4, 123.2 (q, 273 Hz, CF_3), 124.4 (q, 33 Hz, $\mathbf{C}^{4'}CF_3$), 128.8 (q, 5.4 Hz, $\mathbf{C}^{5'}$H), 133.6 (q, 1.6 Hz, $C^{3'}$CO2), 136.1, 153.6, 157.7, 166.0 ^{19}F: δ −59.9	426 381
10c	Cl	111−112	100	^{1}H: δ 3.29 (3H), 4.13 (3H), 7.09 (dd), 7.29 (d), 7.68 (d, 8.3 Hz) ^{19}F: δ −63.6	
10d	NO_2	167−167.5	91	^{1}H: δ 3.34 (3H, SO_2CH_3), 4.18 (3H), 7.51 (dd), 7.74 (d), 7.88 (d) ^{19}F: δ −61.0.	
11	NH_2	143−144	100	^{1}H: δ 3.18 (3H), 4.02 (3H), 4.15 (br 2H s, 3′NH_2), 6.39−6.33 (2H m), 7.29 (d) ^{13}C: δ 40.6, 44.4, 103, 105.0, 106.4, 109.5 (q, 36 Hz), 125 (q, 216 Hz), 128.5 (q, 5.2 Hz), 136.5, 146.2, 154.0, 159 ^{19}F: δ −63.5.	
12a	NHC(O)H	126.5−128.5	58	^{1}H: δ 3.30 (3H), 4.1 (3H), 7.0 (m), 7.14 (0.3H), 7.6 (2H m), 8.25 (0.7H), 8.46 (0.7H), 8.62 (0.3H d, 12.5 Hz) ^{1}H:[b] δ 3.50 (3H), 4.06 (3H), 7.1 (m), 7.4 (0.2H), 7.76 (d, 8.8 Hz), 7.83 (0.8H), 8.35, 9.93 ^{19}F: δ −61.9 (0.9F), −61.4 (2.1F) ^{19}F:[b] δ −55.9 (0.6F), −54.9 (2.4F)	397 255
12b	NHAc	175.5−177.5	93	^{1}H:[b] δ 1.95 (3H, CON**H**), 3.38 (3H, $SO_2C\mathbf{H}_3$), 3.95 (3H, $N^1C\mathbf{H}_3$), 7.04 (dd), 7.20 (d, 2.4 Hz), 7.64 (d, 9.0 Hz), 9.49 (^{1}H s, $C\mathbf{H}_3CO$)	
12c	NHC(O)iPr	143.5−145	93	^{1}H: δ 1.26 (6H d, 6.9 Hz), 2.56 (sept), 3.29 (3H), 4.12 (3H), 6.93 (dm, 8.3 Hz), 7.56-7.59 (2H ∼d), 8.21 (m) ^{19}F: δ −61.6	

Table 1 (Continued)

compd	Q [Z[a]]	mp (°C)	yield (%)	NMR	GC/MS
12d	NHC(O)tBu	100−106	62	^{1}H: δ 1.29 (9H), 3.28 (3H), 4.10 (3H), 6.90 (dd), 7.56 (d, 8.9 Hz), 7.87 (br, CON**H**), 8.22 (d, 2.4 Hz)	
12e	NHC(O)CF_3	117−118	88	^{1}H: δ 3.29 (3H), 4.13 (3H), 7.12 (dd), 7.67 (d, 8.8 Hz), 8.08 (d, 2.4 Hz), 8.26 ^{19}F: δ −77.8, −61.35	465
12f	NHC(O)CH_2Cl	133−134.5	86	^{1}H: δ 3.29 (3H), 4.12 (3H), 4.21 (2H), 7.00 (dd), 7.62 (d, 9.2 Hz), 8.17 (d, 2.0 Hz), 8.84 (br, CON**H**)	445 384 369
12g	NHC(O)CH_2OAc	133.5−134	93	^{1}H: δ 2.23 (3H), 3.29 (3H), 4.12 (3H), 4.71 (2H), 6.97 (dd), 7.60 (d, 8.8 Hz), 8.29 (d, 2.4 Hz), 8.46 (br) ^{19}F: δ −61.6	
12h	NHC(O)CH_2OH	143−144.5	31	^{1}H:[b] δ 3.48 (3H), 4.02 (2H d, 5.5 Hz), 4.05 (3H), 6.27 (tr, 5.5 Hz), 7.04 (dd), 7.75 (d, 8.9 Hz), 7.99 (d, 2.5 Hz), 9.39 ^{19}F:[b] δ −58.9	
12i	NHC(O)CH_2OMe	102−104	85	^{1}H: δ 3.28 (3H), 3.52 (3H), 4.02 (2H, C**H**$_2$OMe), 4.12 (3H), 6.95 (dd, 8.8 and 2.8 Hz), 7.59 (d, 8.8 Hz), 8.31 (d), 8.93 (br, CON**H**) ^{19}F: δ −61.9	
12j	NHC(O)CH_2CO_2Me	131−132	80	^{1}H: δ 3.29 (3H), 3.53 (2H), 3.83 (3H), 4.12 (3H), 6.96 (dm), 7.61 (d, 8.8 Hz), 8.17 (m), 9.74 (br) ^{19}F: δ −62.2	
12k	NHC(O)CONHMe	185−186.5	34	^{1}H: δ 2.89 (3H d, 6.4 Hz), 3.19 (3H), 4.03 (3H), 6.90 (dd), 7.31, 7.54 (d, 12 Hz), 8.16 (d, 3.2 Hz) , 9.77 (s)	
12l	NHCO_2iBu	111−112.5	90	^{1}H: δ 0.96 (6H d, 6.7 Hz), 1.99 (m), 3.29 (3H), 3.95 (2H d, 6.7 Hz), 4.12 (3H), 6.87 (dm), 7.00, 7.55 (d, 8.8 Hz), 8.04 (s) ^{19}F: δ −61.75	469 395c
12m	NHC(=NSO_2CF_3)Me	glass	18	^{1}H: δ 2.15, 2.69 (2H), 3.28 (3H m), 4.13 (3H m), 7.15−7.85 (4H m)	542
12n	NHSO_2CF_3	115.5−117.5	13	^{1}H: δ 3.29 (3H), 4.14 (3H), 7.15 (dd), 7.46 (d, 2.4 Hz), 7.67 (d, 8.9 Hz), 7.89 ^{19}F: δ −80.9 (3F ~q), −64.2 (3F q, 3.6 Hz)	
13a	NMeAc	203−205	75	^{1}H: δ 1.81 (3H), 3.20 (3H), 3.30 (3H), 4.14 (3H), 7.07 (d, 2.4 Hz), 7.26 (dd, 8.8 and 2.4 Hz), 7.76 (d, 8.8 Hz)	
13b	N(Ac)$CH_2C{\equiv}CH$	161.5−164.5	58	^{1}H: δ 1.83 (3H), 2.26 (~tr, 2.4 Hz, C≡C**H**), 3.29 (3H), 3.70 (dd, 17.6 and 2.4 Hz), 4.14 (3H), 5.16 (dd, 17.2 and 2.8 Hz), 7.25 (d), 7.31 (dd), 7.77 (d)	
14	NHOH	141−143	100	^{1}H:[b] δ 4.07 (3H), 6.55 (dd), 6.98 (d), 7.48 (d, 8.8 Hz), 8.67, 8.80 (d, 1.5 Hz) ^{19}F:[b] δ −56.9	
15a	N(Ac)OH	162 (dec)	72	^{1}H:[b] δ 2.12 (3H, br), 3.48 (3H), 4.05 (3H ~d), 7.25 (s), 7.30 (d), 7.80 (d, 8.8 Hz), 10.7 (br s)	
15b	N(Ac)OAc	166−167	80	^{1}H: δ 1.62 (3H), 2.19 (3H), 3.30 (3H), 4.13 (3H), 7.35 (br m), 7.54, 7.77 (d, 8 Hz) ^{19}F: δ −62.5 (1F), −62.1 (1F)	
16a	OEt	129−129.5	5	^{1}H: δ 1.45 (3H tr, 6.9 Hz), 3.28 (3H, SO_2C**H**$_3$), 4.11 (5H, q+s), 6.64 (dd, 8.7 and 1.5 Hz), 6.78 (d), 7.52 (d) ^{19}F: δ −62.9	
16b	OMe	130−134	83	^{1}H: δ 3.26 (3H, SO_2CH_3), 3.87 (3H, OCH_3), 4.09 (3H, N^1CH_3), 6.64 (dd, 8.6 and 2.2 Hz, $C^{6'}$H), 6.79 (d, 2.1 Hz, $C^{2'}$H), 7.49 (d, 8.6 Hz, $C^{5'}$H)	
17	H[CF_3]	yellow oil n_D = 1.4535	89	^{1}H: δ 3.91 (3H q, 1.0 Hz), 7.14 (2H dtr, 9.4 and 2.7 Hz), 7.20 (2H dm, 9.5 Hz) ^{13}C: δ 37.4, 118.4, 122.3, 154.9 ^{19}F: δ −60.0(3F), −61.2 (3F)	
18a	H[SMe]	60.5−62.5	75	^{1}H: δ 2.37 (3H), 3.85 (3H), 7.08 (2H dtr, 8.0 and 2.7 Hz), 7.14 (2H dm, 8.0 Hz) ^{19}F: δ −60.0	
18b	NHAc [SMe]	121−122	90	^{1}H: δ 2.21 (3H, COC**H**$_3$), 2.40 (3H), 3.87 (3H), 6.83 (dd, 9.0 and 3.0 Hz), 7.18 (dq, 9.0 and 1.4 Hz), 7.40 (br), 8.26	
19a	H [SO_2Me]	81−83	100	^{1}H: δ 3.28 (3H), 4.10 (3H), 7.17 (2H dtr, 9.4 and 2.7 Hz), 7.21 (2H d, 9.4 Hz) ^{19}F: δ −59.9	
19b	NHAc [SO_2Me]	142.5−143	62	^{1}H: δ 2.22 (3H), 3.28 (3H, SO_2C**H**$_3$), 4.09 (3H), 6.87 (dd, 9.2 and 2.8 Hz), 7.22 (dq, 9.2 and 1.2 Hz), 7.43 (br), 8.31 (~d) ^{13}C: δ 24.9 (CO**C**H$_3$), 40.6 (N**C**H$_3$), 44.5 (SO_2**C**H$_3$), 102.4 (**C**^{4}Cl), 111.0, 113.0, 121.4, 131.8, 135.8, 154.1, 154.5 ^{19}F: δ −59.5	

[a] See Figure 1 for definitions of Q and Z. [b] Spectra taken in DMSO-d_6 instead of in deuteriochloroform. [c] Secondary peak reflecting partial (18%) decomposition to the isocyanate in the GC injection port.

diazotization and reduction with hypophosphorous acid were less effective.

Fluoronitrobenzotrifluoride (**22a**; Q = H) was commercially available. This was not the case either for nitrotoluate ester **22b** (Q = CO_2R) or for nitrofluoroanisoles **23a** (Q = H) and **23b** (Q = NHAc). Nitration of the commercially available tetrafluoroanisole **26** returned both *m*-nitroanisole **23a** and its *ortho* isomer **27**, with the latter being the major product produced (75%). These isomeric fluoronitroanisoles are too similar in physical properties to be separated chromatographically but have quite different reactivities in aromatic nucleophilic substitution reactions.

To exploit this fact, the mixture of fluoronitroanisoles was reacted with hydroxypyrazole. For both isomers, displacement occurred exclusively *ortho* to the nitro group. Fluoride was displaced readily from **23a** to give a pyrazole anisole ether **25a**. In contrast, trifluoromethoxide displacement from *o*-nitroanisole **27**, to give fluorophenyl ether **28** (Z′ = F), was sluggish. The pyrazole ether products were readily separable from each other and from unreacted **27**. Subsequent reduction, acetylation, and nitration of **27** returned amidonitrofluoroanisole **23b** (Q = NHAc); this compound reacted with hydroxypyrazole to give **25b** (Q = NHAc).

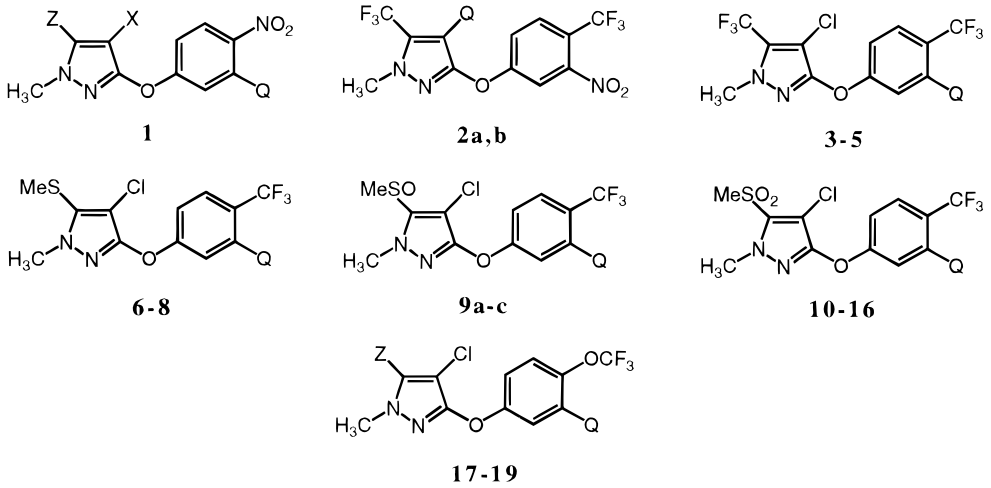

Figure 1. Generic structures for herbicidal pyrazole phenyl ethers cited in this paper.

Scheme 1

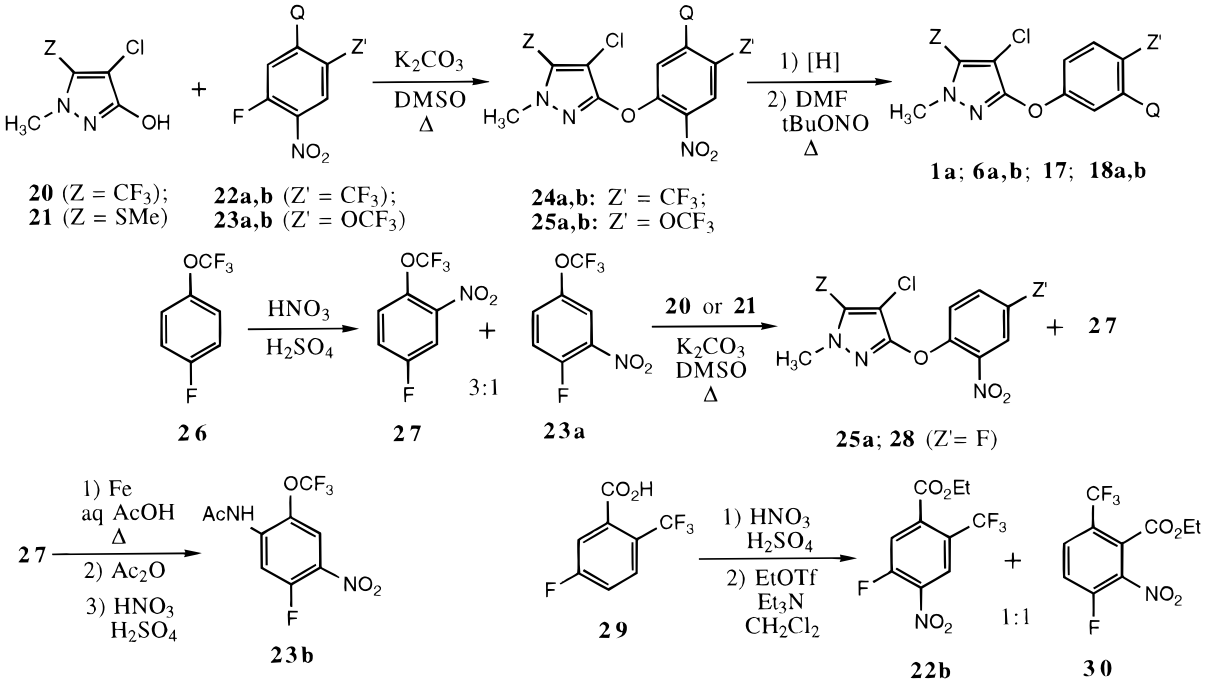

The ester precursor **22b** had to be prepared from fluorotoluic acid **29** (Yarsley). Somewhat surprisingly, nitration was not regioselective. The desired compound was obtained as a 1:1 mixture with its isomer, producing a mixture of **22b** and **30** after esterification. The isomer was carried along through coupling and did not appear to compromise subsequent reduction and deamination reactions appreciably.

Methylthiopyrazole Oxidations. Sulfones **10**, **11**, **16**, and **19** were produced by oxidation of 5-(methylthio)pyrazole ethers **6**−**8** with excess *m*-chloroperbenzoic acid (mCPBA) in dichloromethane. Stoichiometric mCPBA gave sulfoxides, but chromatographic separation from unreacted starting material and sulfone was then required. Oxidation with magnesium monoperoxyphthallic acid (MMPP) in acetic acid (Brougham *et al.*, 1987) gave much cleaner preparations amenable to purification by recrystallization and, therefore, was preferred for preparation of **9a**−**c**. Generally, oxidation was best carried out as early as possible in a synthetic sequence, since sulfonyl and sulfinyl analogs were usually tractable crystalline solids, whereas their thioether precursors were often syrups or glassy solids at room temperature.

α,α,α-Trifluorotoluidide Ethers (Scheme 2). A slightly different approach, which is outlined in Scheme 2, was taken for the synthesis of 3′-amino derivatives of pyrazole tolyl ethers. **22a** was reduced and converted to acetanilide **31**. Nitration afforded a mixture of **32a** and **32b**, which was hydrolyzed and deaminated to give **33**. Overall yield for the sequence was 45−60%, with most losses occurring in the final reductive deamination step.

The *m*-nitro group in **33** is much less activating than is the *o*-nitro group in the isomeric **22a**. Although 5-(methylthio)-hydroxypyrazole **21** reacted cleanly with **33** to give pyrazole tolyl ether **6d**, reaction of **33** with the much less nucleophilic 4-chloro-5-(trifluoromethyl)pyrazole **20** failed to go to completion under the usual conditions. Instead, the 4-unsubstituted pyrazole **34** was used, and the product **1d** was subsequently treated with dibromodimethylhydantoin ($DMHBr_2$) to give 4-bromopyrazole ether **1e**; chlorination of **1d** with dichlorodimethylhydantoin gave **1f**.

The 3′-nitro moiety in **1f** was reduced by hydrogenation over palladium on carbon, but 5-thiomethyl derivatives **6d**, **9b**, and **10d** poisoned the catalyst. Hence the latter nitro ethers were reduced with iron powder in acetic acid. The sulfoxide **9b** was doubly reduced to **34** under these conditions, whereas reduction of thioether **6d** to fluorotoluidine **34** was accompanied by partial acetylation. Hence, neither the pure 3′-amino **34** nor its sulfoxide analogs were isolated. Instead, crude **34** was fully acetylated to produce **7**, which was oxidized to **9c**.

It is essential that pyrazole halogenation be carried out before the (deactivating) nitro group is reduced to an (activat-

Table 2. Biological Activity for Pyrazole *p*-(Trifluoromethyl)- and *p*-(Trifluoromethoxy)phenyl Ethers

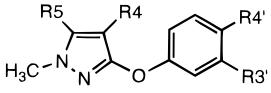

compd	R4′	R3′	R5 (R4)[a]	SRS_{NL}[b]	ED_{80}(NL)[c]	SRS_{BL}	ED_{80}(BL)
12b	CF_3	NHAc	SO_2Me	95.6	1.70	91.9	0.25
10b	CF_3	CO_2Et	SO_2Me	93.2	0.38	72.1	0.82
4b	CF_3	NHAc	CF_3	92.4	3.20	73.6	3.50
12d	CF_3	NHC(O)tBu	SO_2Me	90.0	0.45	93.9	0.25
13a	CF_3	NMeAc	SO_2Me	89.5	1.10	85.6	0.82
9c	CF_3	NHAc	SOMe	89.1	2.70	94.9	0.92
15b	CF_3	N(Ac)OAc	SO_2Me	88.3	1.30	99.2	0.22
6b	CF_3	CO_2Et	SMe	86.5	0.78	54.8	1.10
12k	CF_3	NHC(O)C(O)NHMe	SO_2Me	85.9	0.39	85.3	0.25
12l	CF_3	$NHCO_2iBu$	SO_2Me	85.7	1.40	90.3	1.20
16a	CF_3	OEt	SO_2Me	84.3	1.10	83.2	0.66
10a	CF_3	H	SO_2Me	83.9	1.20	73.7	3.10
12c	CF_3	NHC(O)iPr	SO_2Me	83.4	0.31	87.2	0.20
15a	CF_3	N(Ac)OH	SO_2Me	82.9	0.65	58.1	0.55
12i	CF_3	$NHC(O)CH_2OMe$	SO_2Me	81.6	1.20	79.7	0.46
13b	CF_3	$N(CH_2C{\equiv}CH)Ac$	SO_2Me	80.6	1.10	94.0	0.36
9a	CF_3	H	SOMe	79.8	2.80	62.9	5.00
6a	CF_3	H	SMe	79.0	1.00	83.5	5.10
12a	CF_3	NHC(O)H	SO_2Me	78.4	1.40	87.0	0.22
6d	CF_3	NO_2	SMe	78.1	3.40	64.1	7.00
12j	CF_3	$NHC(O)CH_2CO_2Me$	SO_2Me	77.9	0.31	107.5	0.20
4	CF_3	NMeAc	CF_3	77.6	3.40	68.6	3.20
6c	CF_3	Cl	SMe	75.6	2.60	71.1	4.40
10c	CF_3	Cl	SO_2Me	75.1	2.40	74.9	3.20
5	CF_3	NHMe	CF_3	74.8	0.85	64.1	3.70
11	CF_3	NH_2	SO_2Me	74.1	2.80	60.6	1.90
8	CF_3	OMe	SMe	72.9	0.87	72.5	2.40
9b	CF_3	NO_2	SOMe	71.7	6.10	42.9	5.50
7	CF_3	NHAc	SMe	69.7	4.20	75.6	4.40
12h	CF_3	$NHC(O)CH_2OH$	SO_2Me	66.4	1.60	88.3	1.40
19b	OCF_3	NHAc	SO_2Me	65.9	3.50	49.2	1.50
1f	CF_3	NO_2	CF_3	64.5	3.20	68.7	5.80
12m	CF_3	$NHC(NSO_2CF_3)Me$	SO_2Me	63.2	2.30	84.8	0.97
12g	CF_3	$NHC(O)CH_2OAc$	SO_2Me	62.6	1.50	71.4	1.00
16b	CF_3	OMe	SO_2Me	62.2	3.90	70.3	0.96
2	CF_3	NH_2	CF_3	60.3	3.10	88.7	4.40
1c	CF_3	Cl	CF_3	60.2	0.98	52.7	4.40
12e	CF3	$NHC(O)CF_3$	SO_2Me	59.3	1.90	69.1	1.10
18a	OCF_3	H	SMe	58.2	9.00	55.5	12.00
1b	CF3	Br	CF_3	57.9	3.30	53.2	5.50
19a	OCF_3	H	SO_2Me	57.1	6.20	53.5	5.90
1e	CF_3	NO_2	CF_3 (Br)	56.7	5.20	46.2	6.40
12f	CF_3	$NHC(O)CH_2Cl$	SO_2Me	56.6	5.90	54.8	4.00
10d	CF_3	NO_2	SO_2Me	51.4	16.00	33.3	6.40
12n	CF_3	$NHSO_2CF_3$	SO_2Me	41.4	8.60	79.8	0.99
14	CF_3	NHOH	SO_2Me	40.5	8.40	44.0	5.40
1d	CF_3	NO_2	CF_3 (H)	36.5	7.00	35.7	13.00
1a	CF_3	H	CF_3	30.2	5.40	51.3	6.20
17	OCF_3	H	CF_3	ND[d]	ND	ND	ND
18b	OCF_3	NHAc	SMe	ND	ND	ND	ND

[a] R^4 = Cl unless otherwise indicated. [b] SRS, scaled rank sum: 0 = minimum activity, 100 = maximum. [c] Rate in kg/ha required to achieve an average growth reduction of 80% across warm-season weed species. [d] Not titrated due to low activity in primary testing.

ing) amino group; otherwise, the pyrazole ring is less susceptible to electrophilic attack than is the phenyl ring. This selectivity was exploited in the synthesis of **1b**, for which the bromo group was introduced after reduction of **1f**. The *para*-directing amino group was then readily removed by diazotization in dimethylformamide.

Acyl Derivatives. Acylation of the toluidine ether **11** in refluxing acetonitrile proved a rich source of active analogs (Scheme 2; **12a**−**l** in Table 1). Reaction with triflic anhydride gave the sulfonyl acetamidine **12m** instead of the desired sulfonamide **12n**. The latter compound was successfully prepared, albeit in poor yield (13%), by reaction in dichloromethane. Glycolate **12h** was obtained by hydrolysis of acetoxyacetanilide **12g** with mild base. It is noteworthy that ester cleavage to **12h** (31% yield) was accompanied by extensive hydrolysis of the toluidide bond, giving **11** in 54% yield.

***N*′′-Substituted Toluidines (Scheme 3).** Attempts to alkylate fluorotoluidines such as **2** and **11** directly failed, but the corresponding toluidides **3** and **12b** reacted readily under phase-transfer conditions to give **4**, **13a**, and **13b**. Unfortunately, such tertiary fluorotoluidides proved refractory toward hydrolysis. Only partial (69%) solvolysis at the *N*′′-methyl group in toluidide **4** was evident in methanolic hydrochloric acid even after 3 days at reflux. This was long enough, however, for extensive hydrolysis of the 4′-trifluoromethyl group in the product to take place, affording a 21% yield of anthranilate ether **35** and reducing the yield of the desired *N*′′-methyltoluidine **5** to 44%. Indeed, gas chromatographic analysis of the reaction mixture over time indicated that the solvolysis of the desired fluorotoluidine product proceeds more rapidly than does hydrolysis of the fluorotoluidide starting material.

Hydroxylamine **14** was prepared from 3′-nitro **10d** using borohydride as reductant in the presence of a catalytic amount of elemental selenium (Yanada *et al.*, 1986). Reaction with acetyl chloride returned hydroxamic acid **15a** or *O*-acetyl hydroxamate **15b**, depending on the stoichiometry at which

Scheme 2

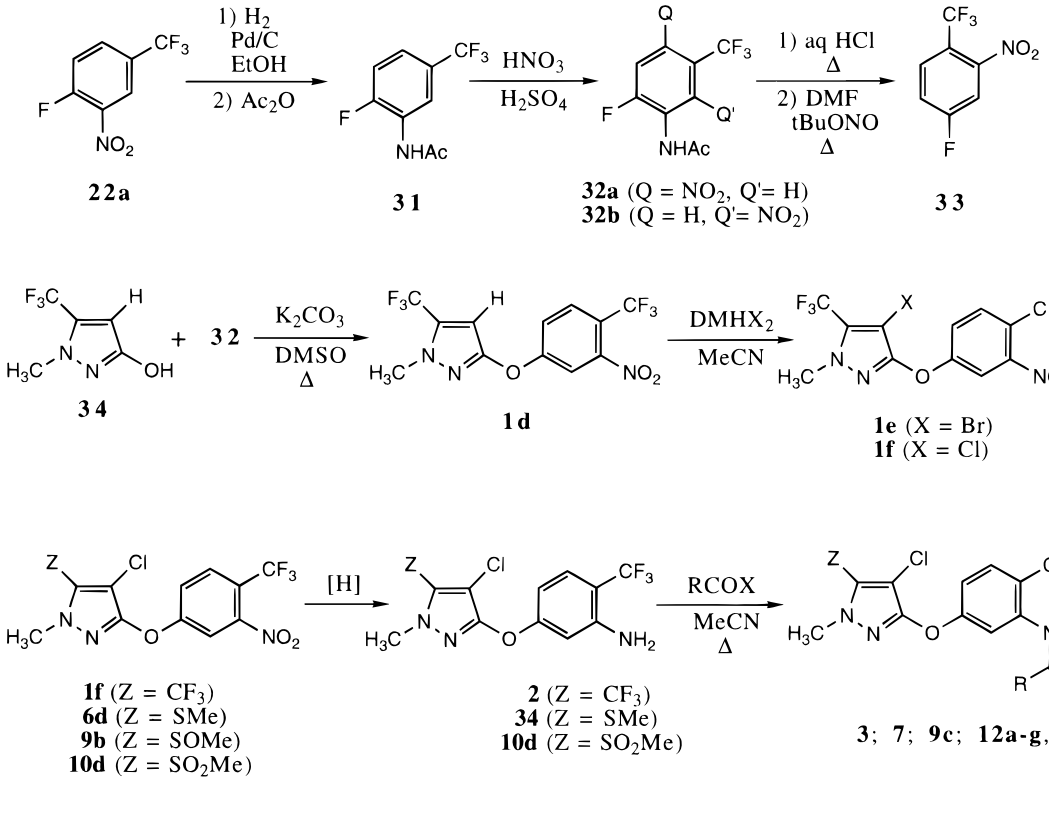

Scheme 3

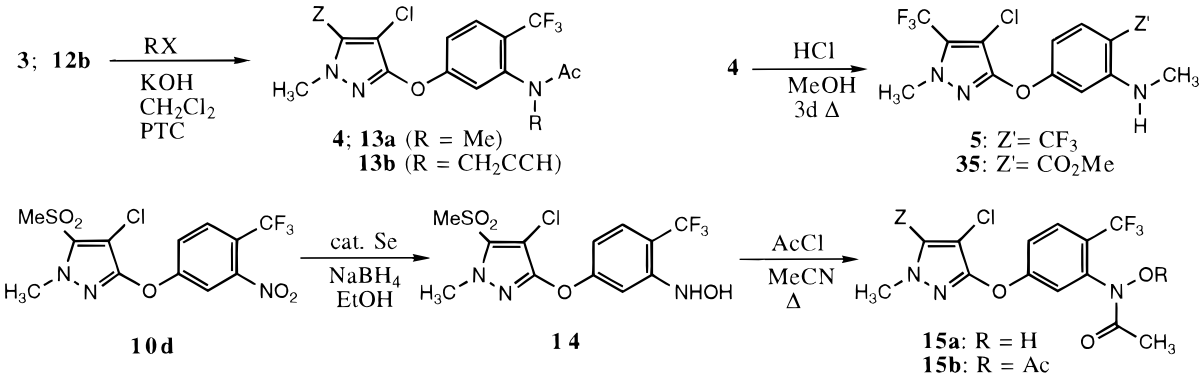

Scheme 4

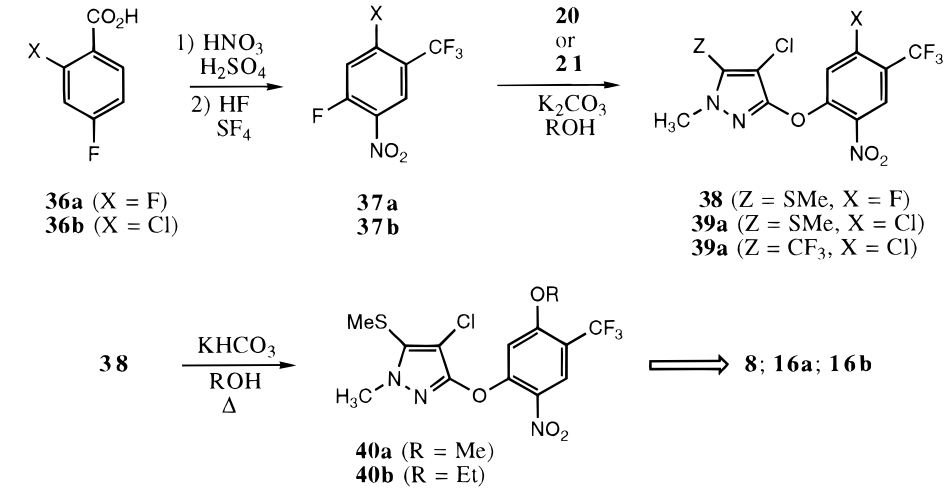

the reaction was run. The diacetylated compound proved surprisingly resistant to solvolysis.

Alkoxy-α,α,α-Trifluorotolyl Ethers (Scheme 4). Many of the most agronomically interesting DPEs and PPEs (e.g., oxyfluorfen and Monsanto's MON 12800, respectively) bear an alkoxy substituent at $C^{3'}$, *i.e., ortho* to the nitro group and *meta* to the ether link. Hence, the analogous pyrazole fluorotolyl ethers were of interest for making a thorough evaluation of

the herbicidal potential of this class of chemistry. In principle, a toluidine ether such as **11** could be converted to the corresponding phenol or methyl ether via diazotization. In practice, however, this compound is too electron deficient to undergo such a reaction. Hence, diazotization goes poorly, and reduced or polymeric products are obtained instead of the desired oxy derivatives.

Instead, commercially available dihalobenzoic acids **36a** and **36b** were nitrated and the products were converted to the corresponding benzotrifluorides **37a** and **37b** by treatment with sulfur tetrafluoride in anhydrous hydrofluoric acid. Coupling of these dihalo intermediates with hydroxypyrazoles was unexpectedly complicated, however. In dimethyl sulfoxide, the desired heterologous diethers **38** and **39** were minor components of the mixtures obtained. Rather, the predominant products found were bispyrazolyl- and bisalkoxy phenylene diethers; the former were more prevalent for difluoro **37a**, whereas the latter were prevalent when chlorofluoro **37b** was used as starting material. A more favorable product distribution was observed in refluxing methanol, but losses to side products were still considerable. When the first displacement step was run at room temperature, however, it was found that reaction to form **38** and **39** was both regiospecific and quantitative.

3′-Chloro **39a** and **39b** proved unsuitable for further aromatic nucleophilic substitution, because the pyrazoloxy group *ortho* to the activating nitro substituent is a better leaving group than is the chloride at the respective *para* position. Fluoro **38**, on the other hand, reacted cleanly in methanol and in ethanol to yield **40a** and **40b**, respectively. Thioether oxidation, nitro reduction, and deamination were then applied where appropriate as outlined in Scheme 1 to return **8**, **16a**, and **16b**. Application of the same procedures to 3′-chloro **40a** and **40b** afforded **1c**, **6c**, and **10c**.

DETAILED SYNTHESES

4-Fluoro-2-nitrobenzotrifluoride (33). Palladium catalyst (10% on carbon, Matheson Coleman & Bell; 0.3 g) was wet with ethanol. 3-Nitro-4-fluorobenzotrifluoride (**22a**; 33 g, 0.16 mol) was added as a solution in 150 mL of additional ethanol and the slurry pressurized to 50 psi overpressure on a Parr hydrogenator. The cell was agitated and repressurized twice over 15 h, and then the reaction mixture was filtered through Celite and partitioned between 2:1 ethyl ether/ethyl acetate and brine. The organic layer was dried with magnesium sulfate and the solvent evaporated to give the aniline as a yellow oil. The aniline was added to 75 mL of acetic anhydride contained in a flask fitted with a water-cooled condenser; reflux was driven by the heat of reaction as the aniline was added. After 3 h, the solution was poured into 750 mL of water and the anilide product **31** was collected by filtration; yield was quantitative.

Nitric acid (71%; 150 mL) was cooled to 0 °C in a saltwater ice bath, and chilled concentrated sulfuric acid (250 mL) was added slowly. Once the nitration mixture had cooled back below 5°C, acetanilide **31** (24.4 g, 0.14 mol) was added gradually over 20 min. The mixture was then quenched into 350 g of ice water. Nitroacetanilide product **32** was recovered by filtration as a pale yellow powder comprised of 2- and 4-nitro isomers in a 1:1 ratio.

The nitroacetanilide **32** were taken up in 200 mL of methanol, 50 mL of 12 N hydrochloric acid was added, and the mixture was heated to reflux for 1 h. After dilution into water, crude nitroanilines were collected by filtration (20.4 g) and additional product was recovered by extraction of the filtrate with ethyl ether. After drying with magnesium sulfate and evaporation of the solvent, the residual red oil (3.0 g) was taken up in ethyl acetate and dried with magnesium sulfate plus silica gel. Removal of solvent by rotary evaporation gave 27.3 g of isomeric fluoronitroanilines (90% overall yield).

Anhydrous dimethylformamide (300 mL) was heated to 65 °C in a dry flask fitted with a reflux condenser, and *tert*-butyl nitrite (23 mL, 0.17 mol) was added. A portion of the nitrotoluidine mixture (26.9 g, 0.12 mol) was then added dropwise as a solution in 150 mL of anhydrous dimethylformamide at a rate just sufficient to sustain nitrogen evolution. The addition funnel was rinsed with 20 mL of dimethylformamide supplemented with 1 mL (7.6 mmol) of *tert*-butyl nitrite. Once gas evolution was complete, the reaction mixture was diluted to 4 L with ice water and 1 L of concentrated hydrochloric acid. Products were recovered by repeated extractions into ethyl ether, and the combined organic layers were washed with saline 4 N hydrochloric acid and then saline and dried with magnesium sulfate to afford **33** as 14 g of yellow liquid (49% yield). A portion (0.56 g) was dried under vacuum for elemental analysis and biological evaluation, yielding 0.48 g of oil, bp 70 °C at 9 torr (dec).

$C_7H_3F_4NO_2$ (209.11), expected: C, 40.21; H, 1.45; N, 6.70%. Found: C, 40.30; H, 1.46; N, 6.65%. NMR: ^{1}H δ 7.66 (dd, J = 8.8 and 5.0 Hz, C^6**H**), 7.42 (dd, J = 7.6 and 2.4 Hz, C^3**H**), and 7.24 (∼trd, J = 6 and 2.6 Hz, C^5**H**); ^{13}C δ 164.3 (d, J = 270 Hz, **C**^{4}F), 130.3 (m, **C**^{6}H), 123.5, 119.7 (d, J = 22 Hz), and 113.3 (d, J = 27 Hz); ^{19}F δ −60.8 (s, C**F$_3$**) and −103.4 (∼q, J = 5.7 Hz).

4-Chloro-1-methyl-5-(methylthio)-3-[3-nitro-4-(trifluoromethyl)phenoxy]pyrazole (6d). (Methylthio)hydroxypyrazole **21** (4.3 g, 24 mmol) was slurried with potassium carbonate (4 g, 30 mmol) in 50 mL of dimethyl sulfoxide, and **33** (5.0 g, 24 mmol) was added. The reaction flask was flushed with nitrogen and stirred at 80 °C in an oil bath for 24 h, at which point the reaction mixture was diluted into 5% aqueous sodium bicarbonate and products were extracted into 1:1 ethyl acetate/ether. The organic layer was washed twice with brine and dried with magnesium sulfate. Recrystallization from methylcyclohexane with a trace of ethyl acetate gave ether **6d** as beige crystals. $C_{12}H_9ClF_3N_3O_3S$ (367.74), expected: C, 39.19; H, 2.47; N, 11.43%. Found: C, 39.37; H, 2.49; N, 11.52%.

4-Chloro-1-methyl-5-methanesulfonyl-3-[3-nitro-4-(trifluoromethyl)phenoxy]pyrazole (10d). A solution of thioether **6d** (1.0 g, 2.6 mmol) in 20 mL of dichloromethane was cooled to 0 °C, and 3-chloroperbenzoic acid (1.5 g, 7 mmol) was added. After 20 min at 0 °C, the flask was allowed to warm to room temperature and stirred for 10 h. The mixture was then quenched into 5% sodium thiosulfate and the organic layer washed with saturated sodium bicarbonate and then with brine. Solvent was evaporated under reduced pressure and the crude product triturated with methylcyclohexane to give sulfone **10d** as a white powder. $C_{12}H_9ClF_3N_3O_5S$ (399.74), expected: C, 36.06; H, 2.27; N, 10.51; S, 8.02%. Found: C, 36.48; H, 2.29; N, 10.25; S, 7.98%.

4-Chloro-1-methyl-5-methanesulfonyl-3-[3-amino-4-(trifluoromethyl)phenoxy]pyrazole (11). Nitrotolyl ether **10d** (9.85 g, 25 mmol) was dissolved with heating in 75 mL of glacial acetic acid diluted with 25 mL of water. Gradual addition of iron powder (6 g, 0.11 mol) over 30 min gave a vigorous exothermic reaction. After 30 min more at 80 °C, the mixture was diluted into water and extracted twice with ethyl ether after acidification with a few milliliters of hydrochloric acid. The pooled organic extracts were filtered through Celite and dried with magnesium sulfate. Evaporation of solvent gave toluidine ether **11** as a white powder in quantitative yield. $C_{12}H_{11}ClF_3N_3O_3S$ (369.76), expected: C, 38.98; H, 3.00; N, 11.36%. Found: C, 39.27; H, 3.05; N, 11.23%.

4-Chloro-1-methyl-5-methanesulfonyl-3-[3-acetamido-4-(trifluoromethyl)phenoxy]pyrazole (12b). Toluidine ether **11** (2.2 g, 6 mmol) was taken up in 10 mL of acetic anhydride and heated to 50 °C; an additional bolus of 10 mL of acetic anhydride was added after 2 h to keep the mixture homogeneous. After 3 h at 50 °C, the mixture was diluted into water. The product acetanilide **12b** crystallized out of solution as a white solid. $C_{14}H_{13}ClF_3N_3O_4S$ (411.79), expected: C, 40.83; H, 3.18; N, 10.20; S, 7.79%. Found: C, 40.90; H, 3.22; N, 10.26; S, 7.79%.

BIOLOGY

Data Reduction. Summary data for pre-emergent herbicidal activities against warm season weeds are given in Table 2. Fluorotolyl and fluoroanisole pyrazole

ethers described herein are listed in order of decreasing activity on narrowleaf species. Data are cited as scaled rank sums (SRS), which are a more robust measure of potency across species than are classical point estimates such as ED_{50}s or ED_{80}s (Duewer and Clark, 1991; Clark *et al.*, 1995).

All treatment growth reduction (GR) scores for analogs were taken from secondary pre-emergence treatments and broken down into sets of three-rate titrations. Where five application rates had been included in a test, the middle rate was duplicated as the top rate for a second triplet. The pooled triplets were then ranked for growth reduction on large crabgrass as the primary criterion for narrowleaf (NL) injury and on morningglory as the primary broadleaf (BL) criterion. Ties on crabgrass were broken by reference to the GR scores for green foxtail or seedling johnsongrass; velvetleaf served as the secondary ranking criterion for broadleaf injury. Ties at this level were broken by reference to the extent of growth reduction observed for barnyardgrass (NL) or for cocklebur (BL). Remaining ties were broken by reference to the application rate and, as a last resort, to a random number generated for each treatment. Reversing the order of the last two criteria had no appreciable effect on the SRS values obtained.

The criteria ran from most sensitive to least sensitive weed species. Hence, ties on crabgrass or morningglory generally arose from complete or nearly complete control (GR = 95−100%). This serves to effectively extend the dynamic range of the titrations. Ranks for each compound were then totaled across rates, and the resulting rank sums were scaled so that 0 is the minimum possible value and 100 is the maximum attainable score for a fixed titration range.

Some values in Table 2 exceed 100 because they represent titrations for more active compounds which were started at 1.12 kg/ha or less and have been corrected for this titration offset. This was possible because scaled rank sums are log-linear with respect to titration rates (Clark *et al.*, 1995). Hence, a given proportional offset in top titration rate r yields a corresponding interval offset in SRS. The slope α of the SRS/log r line was evaluated by comparing offset titration triplets for those examples for which data were available. The mean $\Delta SRS/\Delta \log r$ obtained was 30.2 ± 1.8 (SEM, $n = 23$) for narrowleaf weeds and 31.2 ± 2.3 for broadleaf weeds; the corresponding median values, at 31.5 and 32.0, were not significantly different from each other or from the respective mean slopes. Hence, triplet SRS values for titrations started at 1.1 kg/ha were normalized to an effective rate of 5.6 kg/ha by adding an offset of 31 log(5.6 / 1.12) = 21.7.

Scaled rank sums are also log-linear with the more familiar ED_{50} (Clark *et al.*, 1995). In this case, an SRS value of 100 corresponds to an ED_{50} of about 50 g/ha for both narrow- and broadleaf weeds. The log-linearity factor α for these data is 31 (see above), so an SRS value of 69 ($=100 - \alpha$) implies an ED_{50} of about 500 g/ha (50 × 10) and an SRS value of 38 ($=100 - 2\alpha$) corresponds to an ED_{50} of 5000 g/ha (50×10^2, *i.e.*, 5 kg/ha). Looked at another way, a scaled rank sum difference of 9 implies a roughly 2-fold difference in ED_{50} ($31 \times \log 2 = 9.3$).

For those compounds for which two triplets were available, the two scaled rank sums obtained were averaged. Analysis of variance within such pairs gives a (conservative) estimate of the standard error within tests for scaled rank sums. Here, the residual mean error was ±7.65 for narrowleaf weeds and ±9.44 for broadleaf weeds. Note that these values correspond to ED_{50} errors of $10^{(8.5/31)} = 1.9\times$, in good agreement with the historical reproducibility of Monsanto's herbicide screens (Duewer and Clark, 1991).

General Observations. Fluorotolyl pyarazole ethers were up to 10-fold less potent when applied as post-emergence herbicides than when applied pre-emergence. Moreover, most proved relatively more active (data not shown) against narrowleaf weed species than were the corresponding nitrophenyl ether analogs (Moedritzer *et al.*, 1992). Despite these differences in the spectrum of activity, the nature of the herbicidal injury was very similar for the two classes, including the desiccation and necrosis characteristic of protoporphyrinogen IX oxidase inhibitors (Sherman *et al.*, 1991).

The most active analogs overall were the 5-sulfonyl 3′-amido analogs **9c**, **12b**, and **12d**, with replacement of the anilide hydrogen by a methyl group (**13a**) having relatively little effect on activity (Table 2). It is interesting to note that oxalic diamide **12k** and carbamate **12l** were also among the analogs most active on both narrow- and broadleaf weeds. Carboxylates **6b** and **10b** were significantly less active on broadleaf than on narrowleaf weeds ($\Delta SRS > 9$), as was the 5-trifluoromethyl 3′-amido **4b**. In contrast, malonate amide **12j** was the analog most active on broadleaves yet was relatively much weaker on monocot species. *N*″-Propargyl **13b** and acetyl hydroxamate **15b** showed a spectrum of activity qualitatively similar to that of **12j**.

In general, 5-trifluoromethyl analogs were less active than were 5-methylthio derived compounds, and fluoroanisole ethers were less active than were the corresponding fluorotolyl ethers. The relative activities within particular sets of thioether/sulfoxide/sulfone congeners varied depending upon the substitution at $C^{3'}$. In sharp contrast to the SAR for 4′-nitro PPEs (Moedritzer *et al.*, 1992; Sherman *et al.*, 1991), the carboxylate **6b** and **10b** were more active than were the analogous 3′-methoxy analogs **8** and **16b**. The latter were comparable in activity to 3′-methylamino-, 3′-chloro, and 3′-unsubstituted fluorotolyl ethers.

Comparative Molecular Field Analysis (CoMFA). CoMFA (Cramer *et al.*, 1988) is an alternative, more quantitative way to summarize structure/activity relationships (SARs). In this procedure, molecular structures of analogous compounds are overlaid on a three-dimensional lattice. Correlations of biological activity with variations in electronic and steric field potentials are then evaluated at each lattice point by partial least-squares (PLS) analysis. The mathematical model obtained can be used to predict the activity of an analog not included in the original data set or as a tool for visualizing SAR in three dimensions.

In the present instance, the Sybyl CoMFA package from Tripos, Inc., St. Louis, MO, was used. A molecular structure for each analog was generated in CONCORD (University of Texas at Austin) and the orientation about the ether bond set to a common starting point defined by an angle of 53.8° between the phenyl plane and the *O*-pyrazole bond and an angle of 11.9° between the plane of the pyrazole ring and the *O*-phenyl bond (Figure 2).

Individual structures were "relaxed" in MOPAC 93 (Quantum Chemistry Program Exchange, Indiana University, Bloomington, IN; by Dr. J. J. P. Stewart and Fujitsu Limited, Tokyo, Japan), using an AM1 Hamiltonian with appropriate amide corrections. In all cases,

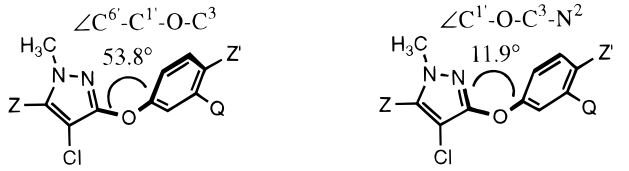

Figure 2. Initial ring configuration from which relaxed pyrazole phenyl ether conformations were derived.

Table 3. Summary Statistics for CoMFA Models Using Scaled Rank Sums (SRS) for Pre-emergence Activity on Narrow- (NL) and Broadleaf (BL) Weeds

response variable	C^a	$\pm SE_x{}^b$	Q^2	P_x	intercept	±SE	±RSE[c]	R^2
SRS_{NL}	5	13.24	0.357	0.06	41.76	6.14	0.15	0.862
SRS_{BL}	3	14.07	0.406	0.02	40.26	8.75	0.22	0.770

[a] C, optimal number of principal components included in the model. [b] Subscript x indicates statistics from leave-one-out cross-validation analyses; $n = 48$. [c] RSE, relative SE of regression (SE/intercept).

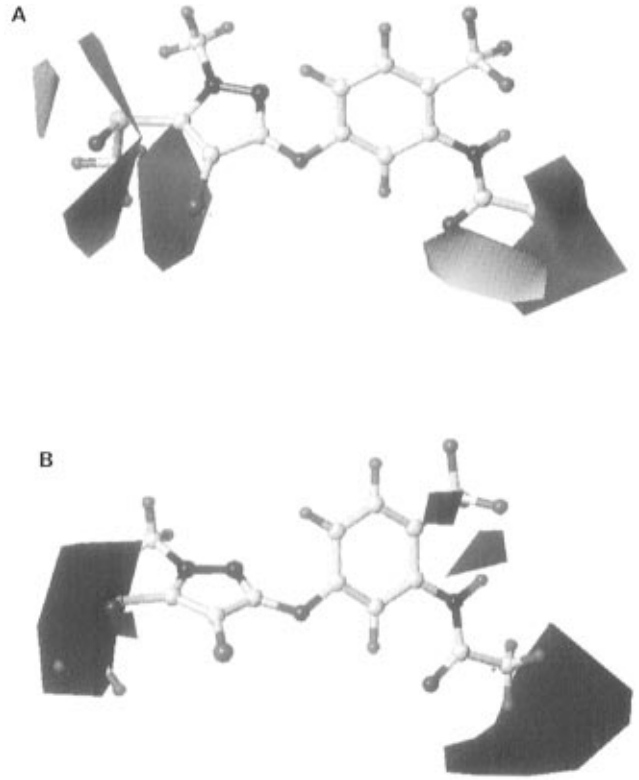

Figure 3. CoMFA maps for narrowleaf activity of trifluorotolyl and trifluoroanisole pyrazole ethers: (A) steric contours at 75% (green; steric bulk is positively correlated with potency) and at 15% (yellow: steric bulk is negatively correlated with potency); (B) electrostatic contours at 75% (blue; electron density is negatively correlated with potency) and at 20% (red; electron density is positively correlated with potency).

the pyrazole group remained in the starting (arbitrarily chosen) quadrant with respect to the phenyl ring. Steric and electronic CoMFA equations were then generated by application of PLS. Some "goodness-of-fit" measures from calculations for narrow- and broadleaf weeds are given in Table 3.

The R^2 value indicates how much of the data set's variation is accounted for by the model, whereas the cross-validated R^2 (Q^2; Cramer *et al.*, 1988) indicates how well biological activity is predicted for each compound by the other analogs in the data set. The Q^2 values obtained here (0.357 and 0.406) are statistically significant but indicate that the models obtained are

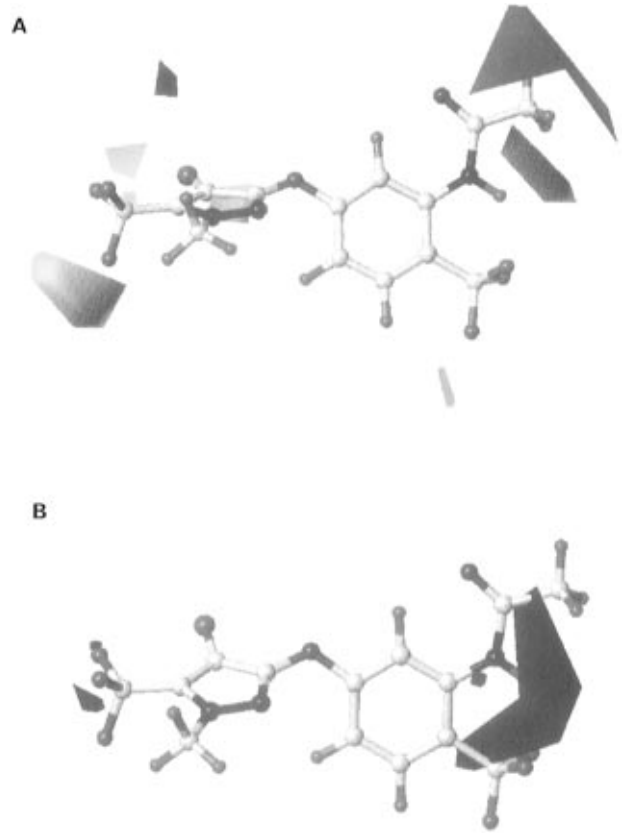

Figure 4. CoMFA maps for broadleaf activity of trifluorotolyl and trifluoroanisole pyrazole ethers: (A) steric contours at 85% (green; steric bulk is positively correlated with potency) and at 20% (yellow; steric bulk is negatively correlated with potency); (B) electrostatic contours at 85% (blue; electron density is negatively correlated with potency) and at 20% (red; electron density is positively correlated with potency).

only modestly predictive (Cramer *et al.*, 1988). It may be possible to enhance the predictivity of the CoMFA models by, for example, identifying outliers and optimizing alignments, though such detailed analyses are beyond the scope of the present work. Standard errors of regression (RSE) were close to the expected noise level (SE ±7−9, see above), indicating that the models are not overspecified.

The CoMFA models are particularly useful in the present instance as a mechanism for providing graphical SAR summaries in the form of 3D contour plots such as those shown in Figures 3 and 4 for narrow- and broadleaf activities, respectively. The steric CoMFA results are shown in Figures 3A and 4A, whereas Figures 3B and 4B show the respective electronic maps. In the latter, blue indicates areas in which increasing electronegativity tends to reduce herbicidal activity, whereas red indicates areas for which greater activity is associated with higher electron density. For the steric maps, green and yellow shadings indicate a positive or negative correlation, respectively, between steric bulk and biological activity.

A large electropositive lobe and favorable steric regions are evident near the pyrazole C^5 substituent in the narrowleaf maps (Figure 3); both are absent in the broadleaf CoMFA maps (Figure 4). (For clarity of presentation, the frame of reference for Figure 4 has been rotated with respect to that of Figure 3. Toluidides **9c** and **3** have been embedded in the CoMFA maps to help orient the reader.) Indeed, in the latter case, sterically prohibitive lobes are evident at this position. This reflects the qualitative difference in spectra dis-

cussed above between bulky, electropositive sulfur in SO_nCH_3 substituents and the relatively compact, electronegative fluorines in a trifluoromethyl group.

Both maps bear an electropositive lobe in the area of the $C^{3'}$ position. The difference between the two maps is subtle and therefore illuminating. The electropositive lobe surrounds the acyl α carbon for narrowleaf weed activity (Figure 3A), whereas in the broadleaf map it envelops the N″ and $C^{4'}$ substituents. For both weed classes, increased steric bulk is favored at the a carbon, but only to a point (*i.e.*, nearly contiguous green and yellow steric areas are evident in this region). These observations suggest that thioalkyl or sulfonyl substitutions might have been advantageous there.

ACKNOWLEDGMENT

Drs. Kurt Moedritzer and Pana Charumilind provided advice and indispensable professional support while this work was being carried out at Monsanto Co. Suggestions made by reviewers of the original manuscript were helpful and are duly appreciated.

LITERATURE CITED

Barton, J. E. D.; Collins, D. J.; Cox, J. M.; Griffin, D. A.; Parry, D. R.; Cartwright, D. ICI Industries, U.S. Pat. 4,738,711, 1988.

Brougham, P.; Cooper, M. S.; Cummerson, D. A.; Heaney, H.; Thompson, N. Oxidation reactions using magnesium monoperphthalate: a comparison with *m*-chloroperoxybenzoic acid. *Synthesis* **1987**, 1015−1017.

Clark, R. D. Synthesis of protoporphyrinogen oxidase inhibitors. In *Porphyric Pesticides*; ACS Symposium Series 559; Duke, S. O., Rebeiz, C. A., Eds.; American Chemical Society: Washington, DC, 1994; pp 34−47.

Clark, R. D.; Parlow, J. J.; Brannigan, L. H.; Schnur, D. M.; Duewer, D. L. Applications of scaled rank-sum statistics in herbicide QSAR. In *Classical and Three-Dimensional QSAR in Agrochemistry*; ACS Symposium Series 606; Hansch, C. Fujita, T., Eds.; American Chemical Society: Washington, DC, 1995; pp 264−281.

Cramer, R. D., III; Patterson, D. E.; Bunce, J. D. Comparative molecular field analysis (CoMFA). *J. Am. Chem. Soc.* **1988,** *110*, 5959−5967.

Doyle, M. P.; Dellaria, J. F., Jr.; Siegfried, B.; Bishop, S. W. Reductive deamination of arylamines by alkyl nitrites in *N*,*N*-dimethylformamide. *J. Org. Chem.* **1977**, *42*, 3494−3498.

Duewer, D. L.; Clark, R. D. Rank-order analysis for robust multi-response, multiblock comparisons: evaluations of herbicide interactions. *J. Chemom.* **1991**, *5*, 503−521.

Hiraga, K.; Shibayama, S.; Yanai, I.; Harada, T. Nihon Nohyaku Co., Ltd., U.S. Pat. 4,226,616, 1980.

Moedritzer, K.; Allgood, S. G.; Charumilind, P.; Clark, R. D.; Gaede, B. J.; Kurtzweil, M. L.; Mischke, D. A.; Parlow, J. J.; Rogers, M. D.; Singh, R. K.; Sikes, G. L.; Weber, R. K. Novel pyrazole phenyl ether herbicides. In *Synthesis and Chemistry of Agrochemicals III*; ACS Symposium Series 504; Baker, D. R., Fenyes, J. G., Steffens, J. J., Eds.; American Chemical Society: Washington, DC, 1992; pp 147−160.

Nandihalli, U. B.; Duke, M. V.; Ashmore, J. A.; Musco, V. A.; Clark, R. D.; Duke, S. O. Enantioselectivity of protoporphyrinogen oxidase-inhibiting herbicides. *Pestic. Sci.* **1994**, *40*, 265−277.

Rogers, M. D.; Moedritzer, K. Monsanto Co., U.S. Pat. 4,964,895, 1990.

Sherman, T. D.; Duke, M. V.; Clark, R. D.; Sanders, E. F.; Matsumoto, H.; Duke, S. O. Pyrazole phenyl ether herbicides inhibit protoporphyrinogen oxidase. *Pestic. Biochem. Physiol.* **1991**, *40*, 236−245.

Yanada, K.; Yamaguchi, H.; Meguri, H.; Uchida, S. Selenium-catalysed reduction of aromatic nitro copmpounds to *N*-arylhydroxylamines. *J. Chem. Soc., Chem. Commun.* **1986**, 1655−1666.

Received for review March 26, 1996. Revised manuscript received July 10, 1996. Accepted August 21, 1996.[⊗]

JF9601978

[⊗] Abstract published in *Advance ACS Abstracts*, October 1, 1996.